Synthesis of Zirconia 1-D Nanomaterials from Local Zircon-Based Zr(OH)$_4$ mediated by PEG-6000

Septawendar Rifki[1,2*], **Nuruddin Ahmad**[1], **Maryani Eneng**[2], **Sutardi Suhanda**[2]
and Purwasasmita Bambang Sunendar[1*]
1. Laboratory of Advanced Material Processing, Department of Engineering Physics, Faculty of Industrial Technology, Institut Teknologi Bandung, Jl. Ganesha 10, Bandung 40132, INDONESIA
2. Department of Advanced Ceramics, Glass and Enamel, Center for Ceramics, Ministry of Industry of Indonesia, Bandung 40272, INDONESIA
*rifkiseptawendar@gmail.com, purwa@tf.itb.ac.id

Abstract
Zirconia 1-D nanomaterials are promising materials that demonstrate extraordinary and unique properties that can be applied in many great fields such as electronic, medical and chemical. The present study reports the synthesis of zirconia 1-D nanomaterials from local zircon-based zirconium hydroxide hydrates mediated with polyethylene glycol 6000 as a structure-directing template. The synthesis was carried out by an aging ultrasonic method at various PEG/Zr mole ratios from 0.067 to 0.167, at pH 9, at a temperature of 80°C and with aging periods for 1-3 hours. Thermogravimetric and Differential Thermal Analysis (TG-DTA) were conducted to identify the thermal behavior of the as-synthesized zirconia and an X-ray diffraction study was used to characterize the mineralogy of the zirconia. Meanwhile, scanning and transmission electron microscopes were used to observe the morphology of the synthesized zirconia.

It was found that the crystallization of zirconia occurred at a temperature of approximately 810°C. However, zirconia 1-D nanomaterials were obtained at a PEG/Zr mole ratio of 0.167 with an aging period of 2 hours and at a calcination temperature of 900°C. The calcined zirconia exhibits good crystallinity and consists of 64.2% and 35.8% of tetragonal and monoclinic phases respectively with the average crystal sizes of less than 20 nm. Besides, the ZrO$_2$ shows 1-D morphologies such as nanorod-like shapes with aspect ratios of 4-12, nanobar-like shapes and elongated agglomerates.

Keywords: Local zircon-based Zr(OH)$_4$, 1-D nanomaterials of ZrO$_2$, PEG-6000, a 1-D structure-directing template, a PEG/Zr mole ratio.

Introduction

Recently, the study of one dimensional (1-D) nanomaterial has gained more interest of scientists and researchers because of its excellent properties such as possessing a high specific surface area, a high porosity, high mechanical strength and high toughness[1-4]. For example, zirconia (ZrO$_2$) 1-D nanomaterial is now considered as a sophisticated material that showcases unique properties and can be applied in sensors, catalysts, or serves as a reinforced element in biomaterial composites, etc.[1,5-8] in many great fields, inter alia, in electronic, chemical and medical.

Various methods have been developed in the preparation of ZrO$_2$ 1-D nanomaterials, including a sol-gel method[8], a deposition method[9], a chemical route[10], anodization processing[11], a hard-template method[12], hydrothermal processing[13], an electrospinning technique[5] etc. However, those methods basically used organometallic compounds, salts and Zr metal as zirconium precursors and would commonly apply specific instruments.

In this study, a facile method using an economical precursor of local zircon-based Zr(OH)$_4$ mediated by PEG-6000 was proposed to synthesize ZrO$_2$ 1-D nanomaterials. Meanwhile, the organic polymer of PEG 6000 was used as a 1-D structure directing template. An aging process along with ultrasound treatment was carried out in the synthesis. The treatment aimed to minimize the particle's contact resulting in non-agglomerated particles[4].

Our previous studies had successfully prepared 1-D nanomaterial of γ-Al$_2$O$_3$ via an ultrasonic aging technique assisted by organic polymers such as PEG[4] and starch[14]. Their works were for the aim to study the effects of aging process, temperature and the composition ratio of an organic polymer template/Al on the characteristics of the resulted γ-alumina1-D nanomaterial by an ultrasonic aging technique.

In addition, the treatment of the ultrasonic irradiation during the synthesis of γ-Al$_2$O$_3$ 1-D nanomaterial has led to the formation of a homogenous morphology of γ-Al$_2$O$_3$ nanofibers[4] and hundreds of nanometers long γ-Al$_2$O$_3$ rods[14].

In this study, ZrO$_2$ 1-D nanomaterials were synthesized from local zircon-based Zr(OH)$_4$ precursor mediated by PEG-6000 at various PEG-6000/Zr ratios through ultrasound treatment at different aging periods. The Zr(OH)$_4$ precursor used is produced from local ZrSiO$_4$ via a modified sodium carbonate sintering technology in our previous study and has a formula of Zr(OH)$_4$•xH$_2$O [15]. The hydrate molecules of the precursor assumed will obstruct the hydrogen bond interaction between the $(-OH^-)$ groups of the precursor and the $(-O-)$ groups of PEG-6000, resulting in ZrO$_2$ not in a 1-D microstructure. Therefore, the ultrasound treatment is assumed to dissipate the hydrates from the Zr(OH)$_4$ structure during the synthesis of ZrO$_2$ 1-D nanomaterials, allowing the

Research Journal of Chemistry and Environment_____Vol. **22(Special Issue II)** August **(2018)**

Res. J. Chem. Environ.

hydrogen bond interaction between the precursor and PEG-6000. The objectives of this study are to synthesize ZrO_2 1-D nanomaterials from local zircon-based $Zr(OH)_4 \bullet xH_2O$ with PEG as a 1-D structure-directing template by an ultrasound treatment; to investigate the thermal behavior and phase transformation and the infra-red spectra of the as-synthesized ZrO_2 and to observe the effect of the PEG/Zr ratios and aging periods on the resulted microstructures of ZrO_2.

Material and Methods

Materials and Instruments: The materials used in this study were local zircon-based $Zr(OH)_4 \bullet xH_2O$ (containing 83.19 wt. % ZrO_2, 5.13 wt. % SiO_2, 0.978 wt. % HfO_2 and 4.61 wt. % LOI at 800 °C) produced from local $ZrSiO_4$ via a modified sodium carbonate sintering technology[15] and PEG-6000 obtained from a local chemical market. All materials were used without further purification. Meanwhile, the apparatus and the instruments used were a thermoscientific cimarec stirring hot plate, an elmasonic E 100 H ultrasonic bath and a Nabertherm electrical furnace with a maximum temperature of 1500°C.

Synthesis of ZrO_2 1-D Nanomaterials from Local Zircon based $Zr(OH)_4 \bullet xH_2O$: Zirconia 1-D nanomaterial was synthesized from local zircon-based $Zr(OH)_4 \bullet xH_2O$ mediated with PEG-6000 at various PEG-6000/Zr mole ratios through an aging ultrasonic method. The parameter conditions in synthesis of ZrO_2 1-D nanomaterials were specified as follows[4]:

- The PEG 6000/Zr mole ratios of 0.067, 0.133 and 0.167 at pH 9 and a temperature of 80 °C with an aging period for 2 hours, labeled as samples A, B2 and C respectively.
- The PEG 6000/Zr mole ratio of 0.133 at pH 9 and a temperature of 80 °C with aging periods for 1, 2 and 3 hours, labeled as samples B, B2 and B3 respectively.

In this study, $Zr(OH)_4 \bullet xH_2O$ was used as a ZrO_2 precursor exhibiting a pH of 9. The ZrO_2 precursor was mixed with PEG-6000 under heating at 80°C in an ultrasonic bath for 2 hours. Then, the as-synthesized ZrO_2 was chilled naturally to room temperature, bearing in solid white products. The final products were filtered, washed with distilled water for several times and then dried in air. The dried products were thermally investigated by a Thermogravimetric and Differential Thermal Analysis (TG-DTA) method. Then, calcination process of the as-synthesized ZrO_2 was conducted in accordance with the TG-DTA results.

Thermal behavior investigation: The thermal behavior of the as-synthesized ZrO_2 was investigated using a Simultaneous TGA-DTA-96 Line instrument.

Functional groups elucidation: The infra-red spectra of the as-synthesized and the calcined zirconias were characterized using a Prestige 21 Shimadzu Fourier Transform Infra-red (FT-IR) Spectrophotometer.

Mineralogy identification: The phases of zirconia were investigated by a PW 1710 X-ray Diffraction (XRD) instrument at 40 Kv and 30 mA with Cu/Kα (λ = 1.54060 Å) radiation source. The diffraction patterns were scanned from 10.000 to 89.980 (2θ) with a step size of 0.020. The phase composition and the crystal size of the calcined ZrO_2 were quantified using a XRD software and estimated by the Scherer equation[15] respectively:

$$D = \frac{K\lambda}{\beta \cos \theta} \qquad (1)$$

where D is the crystallite size, K is a shape factor with a value of 0.9-1.4, λ is the wavelength of the X-rays (1.54056 Å), θ is the Bragg angle and β is the value of the full width at half maximum (FWHM).

Microstructure analysis: The morphology of the calcined ZrO_2 was analyzed using a JEOL JSM-35C scanning electron microscope (SEM) and a JEM-1400 120 kV transmission electron microscope (TEM).

Results and Discussion

Thermal behavior of the as-synthesized ZrO_2: Based on the TG-DTA investigation, the thermal behavior of the as-synthesized ZrO_2 is as shown in figure 1.

The TGA result in figure 1 shows a gradual decrease in weight in the as-synthesized ZrO_2 at about 9% during thermal treatment between 200° and 328 °C, suggesting the evaporation of water molecules. This phenomenon is also explained by an endothermic peak that was observed at 328°C as given by the DTA result.

A huge weight loss in the as-synthesized ZrO_2 at around 47% is spotted from 328° to 752°C, considering the decomposition of the organic polymer PEG-6000. This weight loss is confirmed by exothermic peaks beginning at 436 °, 666 ° and 734 °C and an endothermic peak at 654 °C, that are expected following the gradual degradation of PEG-6000, as shown by the DTA result. Since $Zr(OH)_4$ compounds are mixed with PEG-6000, it was found that two different interactions were established on the surface of PEG-6000 in which the degradation of PEG-6000 occurred[16].

The first one is the interaction between the PEG surface and air and the other is the interaction between PEG and metal zirconium hydroxides. The first interface leads to the exothermic thermooxidative degradation of PEG-6000 as shown by the first exothermic peak starting at 436 °C. When the PEG was in contact with air, it reacted with oxygen to form α-hydroperoxides[16,17] that is thermally labile, resulting in unstable radical hydrocarbons[17]. Meanwhile, an endothermic peak at 654 °C is closely related with the pyrolysis of the PEG that contacted with Zr, leading to heat

*Research Journal of Chemistry and Environment*_____Vol. **22(Special Issue II)** August **(2018)**

Res. J. Chem. Environ.

absorption. The degradation of PEG simultaneously continued at 666 ° and 734 °C. An exothermic peak starting at 734 °C is possibly associated with combustion of the residual carbonaceous material of the degraded PEG.

According to the DTA result in figure 1, zirconia is found to crystallize at approximately 810°C. Another exothermic peak beginning at 900 °C and an endothermic peak starting at 1060°C could be corresponding to the zirconia crystal evolution and phase transformation respectively. The metastable tetragonal ZrO_2 has a lower crystallization temperature than the monoclinic ZrO_2. The exothermic peak at 810°C is assumed as the crystallization temperature of the metastable tetragonal ZrO_2. Therefore, calcination of the as-synthesized ZrO_2 was conducted at 900°C.

Phase transformation of the as-synthesized ZrO_2: Figure 2 presents a XRD pattern of the as-synthesized ZrO_2 at 900°C. The calcined ZrO_2 contains 64.2% of the t-ZrO_2 and 35.8% of the m-ZrO_2 phases. The t-ZrO_2 is identified at diffraction angles 2θ of 30.28°, 50.38° and 60.28°, originating from the (1 0 1), (1 1 2) and (2 1 1) crystal planes, which are specific for the tetragonal structure (PDF2. 830944). Meanwhile, the main peaks of m-ZrO_2 appeared with low intensities at diffraction angles 2θ of 28.34 and 60.28°, dealing with the ($\bar{1}11$) and (111) crystals planes of the monoclinic structure (PDF2. 791771).

Both the t- and the m-ZrO_2 phases emerged with broadened peaks in the XRD pattern indicating that the calcined ZrO_2 consists of very fine crystals. The average crystal sizes of the t- and the m-ZrO_2 were estimated using the Scherer equation assisted by a XRD software. According to the Scherer equation, the average crystal sizes of the (1 0 1), (1 1 2) and (2 1 1) main crystal planes of the t-ZrO_2 are 16 nm, 10 nm and 13 nm respectively (figure 2). In addition, the m-ZrO_2 also exhibits crystals in nanometer size, such as 16 and 4 nm corresponding to the ($\bar{1}11$) and (111) crystals planes respectively.

FT-IR spectra characteristics of the as-synthesized and the calcined ZrO_2: The detailed FT-IR spectra of the origin as-synthesized ZrO_2 and the calcined ZrO_2 at 900°C as displayed in figure 3 shows that the FT-IR spectra is in the range from 4000 cm^{-1} to 400 cm^{-1}. The FT-IR spectra demonstrate the vibration modes of chemical bonds on the $Zr(OH)_4$-PEG samples. The FT–IR spectrum of the ultrasonically treated as-synthesized ZrO_2 at 80°C consisting of a $Zr(OH)_4$ and PEG-6000 mixture is shown at the bottom of figure 3. Some vibration modes of chemical bonds on the PEG-6000; however, overlap with the metal and oxygen bonds as well as some of the overlapped vibration modes on Zr-O and Si-O bonds. The elucidation of the FT-IR spectra peaks of the (A) as-synthesized ZrO_2 and (B) the calcined ZrO_2 at 900°C is given in table 3.[4,16,18-26]

Figure 3 also shows the profile change on the ZrO_2 spectra to temperature. The main differences between the FT-IR spectra of the as-synthesized ZrO_2 and that of the calcined ZrO_2 at 900°C are all vibration peaks of chemical bonds corresponding to the polymers disappeared, the profile of peaks at around 1100 and 1600 cm^{-1} weakened and the absorption peaks of metal and oxygen bonds significantly sharpened in finger print.

In this study, an organic polymer of PEG-6000 was used as a 1-D structure-directing template. Thus, it was assumed that this might lead to the formation of 1-D ZrO_2 structures in the synthesis. However, since PEG is reacted with the ZrO_2 precursors in the synthesis, there are two possible mechanisms that occurred during the said interaction. The first possible mechanism is the interaction between PEG and the zirconia precursor [$Zr(OH)_4$] through intermolecular hydrogen bonding of the ether groups (-O-) in a PEG structure with the hydrogen of hydroxyl groups of the precursors[4]. This phenomenon is confirmed by a weak band that is recorded as a shoulder at around 3235 cm^{-1}.

Another interaction between PEG and the ZrO_2 precursors perhaps occurred through coordinate covalent bonding from sharing the lone pair e^- of the ether groups (-Ö-) in a PEG structure to the metal ions of Zr^{4+} which is stronger than hydrogen bonding.

According to the FT-IR spectra of the as-synthesized ZrO_2 in figure 3, a band of the hydrate molecules in the $Zr(OH)_4$ structure is not detected at around 1400cm^{-1}.[15] Thus, the ultrasound treatment successfully dissipates the hydrate molecules from the precursor structure, leading to direct interaction of the hydrogen bonding between the $(-OH^-)$ groups of the precursor and the $(-O-)$ groups of PEG-6000. The possible interactions between the PEG and $Zr(OH)_4$ can be assumed as shown in figure 4. These interactions are expected to facilitate the 1-D structure direction of ZrO_2 by PEG-6000.

Microstructure analysis by SEM and TEM: Figure 5 (A, B2 and C) shows typical SEM images of the ZrO_2 microstructures prepared at various PEG/Zr ratios and calcination at 900°C. In this study, the amount of PEG added was 0.067 (A), 0.133 (B) and 0.167 (C) over the Zr precursor's mole. According to figure 5 (A, B2 and C), the addition of PEG at all the PEG/Zr mole ratios has led to the formation of ZrO_2 particles mostly in a rod-like structure, especially at the PEG/Zr mole ratios of 0.133 and 0.167 (see the SEM images of samples B2 and C in figure 5 respectively). Large rod-like particles of ZrO_2, however, with a diameter of 260 nm and 1 μm in length and a diameter of 110 nm and 850 nm in length are obviously observed in samples B2 and C respectively.

In addition, more rod-like ZrO_2 particles can be found in sample C. The PEG/Zr mole ratio of 0.167 seems to be the optimum amount to produce ZrO_2 particles in a 1-D structure from $Zr(OH)_4$. Based on figure 5 (A, B2 and C), it can be concluded that the higher is the PEG/Zr mole ratio used, the

*Research Journal of Chemistry and Environment*_____Vol. **22(Special Issue II)** August **(2018)**

Res. J. Chem. Environ.

more rod-like particles of ZrO_2 are formed. It is also then assumed that the higher is concentration of PEG added, the higher the chance of interaction between PEG and $Zr(OH)_4$ will occur during synthesis leading to better templating process of the ZrO_2 precursors by PEG.

A sample B that applied the PEG/Zr mole ratio of 0.133 in the synthesis of 1-D ZrO_2 nanomaterials was selected to study the effect of aging periods on its microstructure. Figure 5 (B, B2 and B3) shows the microstructures of ZrO_2 particles synthesized by ultrasound treatment with PEG-6000 as a 1-D structure-directing template at different aging periods of 1 hour, 2 hours and 3 hours respectively. A sample B of ZrO_2 that was synthesized at a temperature 80°C for 1 hour had some rod-like particles in its microstructure as given by SEM in figure 5B. Meanwhile, when the aging period was longer at about 2 hours, more rod-like ZrO_2 particles grew and two rod-like ZrO_2 particles with diameters below 500 nm and 1 μm in length were clearly observed (figure 5B2).
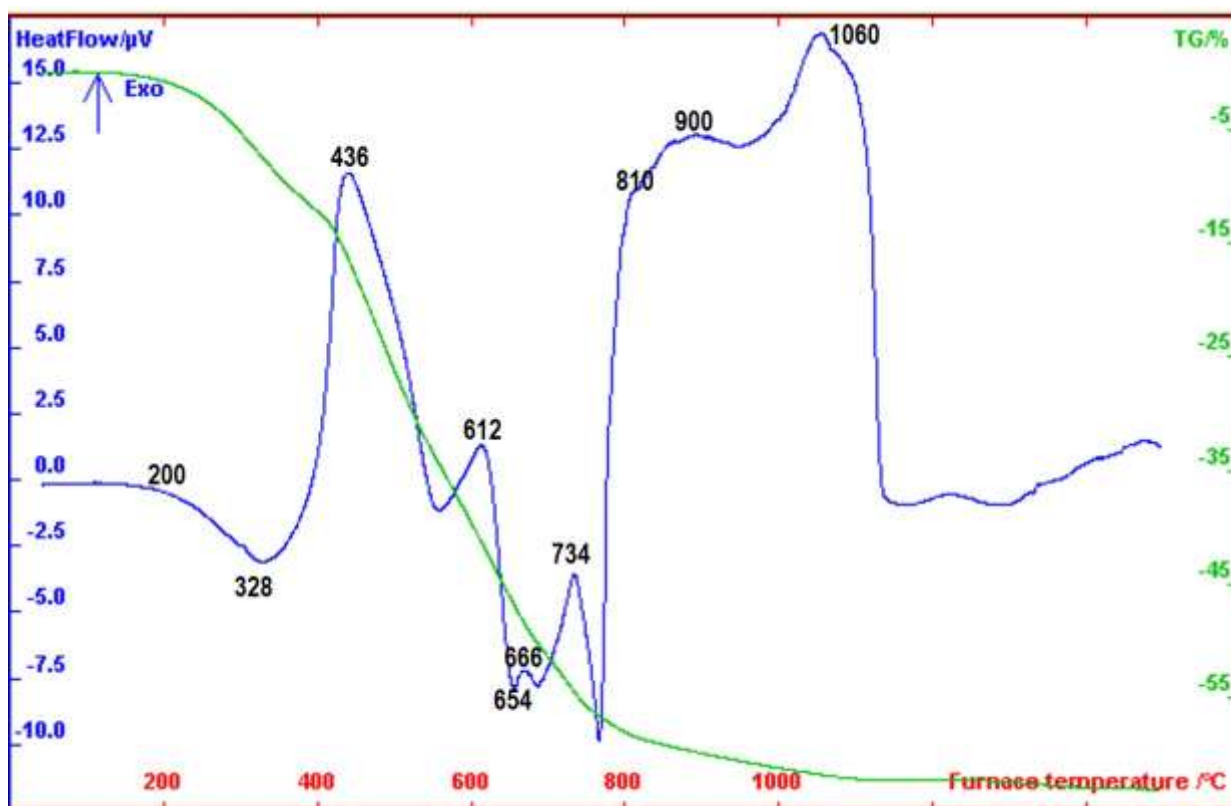
Figure 1: The TG-DTA results of the as-synthesized ZrO_2 during the thermal treatment
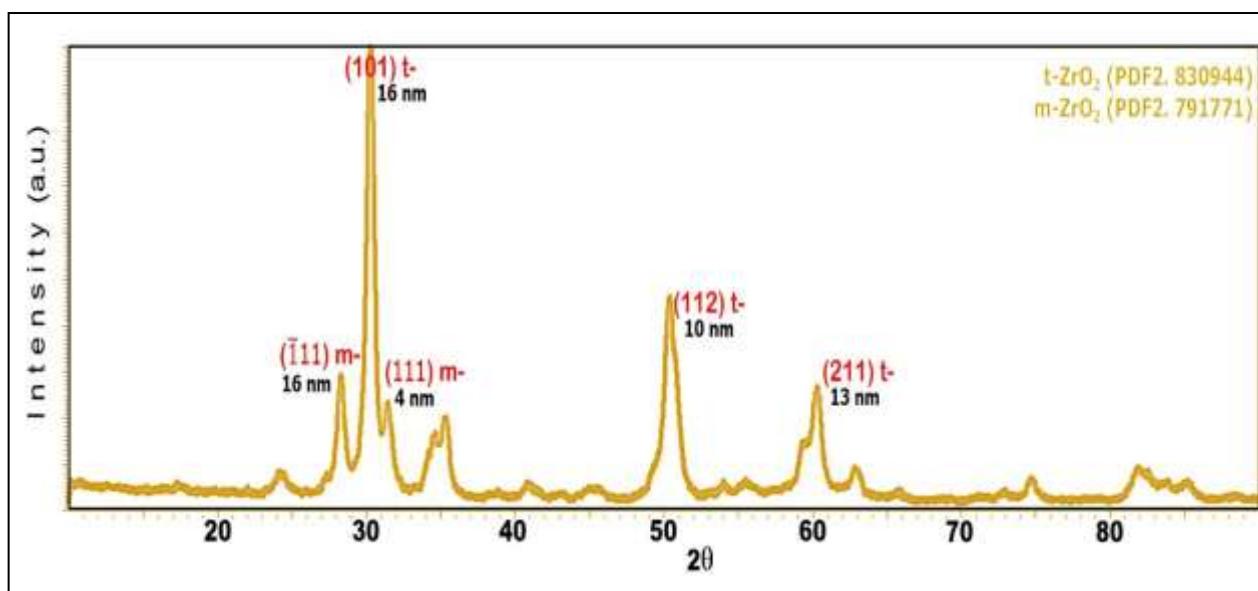
Figure 2: The XRD patterns of ZrO_2 at 900 °C

*Research Journal of Chemistry and Environment*_____Vol. **22(Special Issue II)** August **(2018)**

Res. J. Chem. Environ.
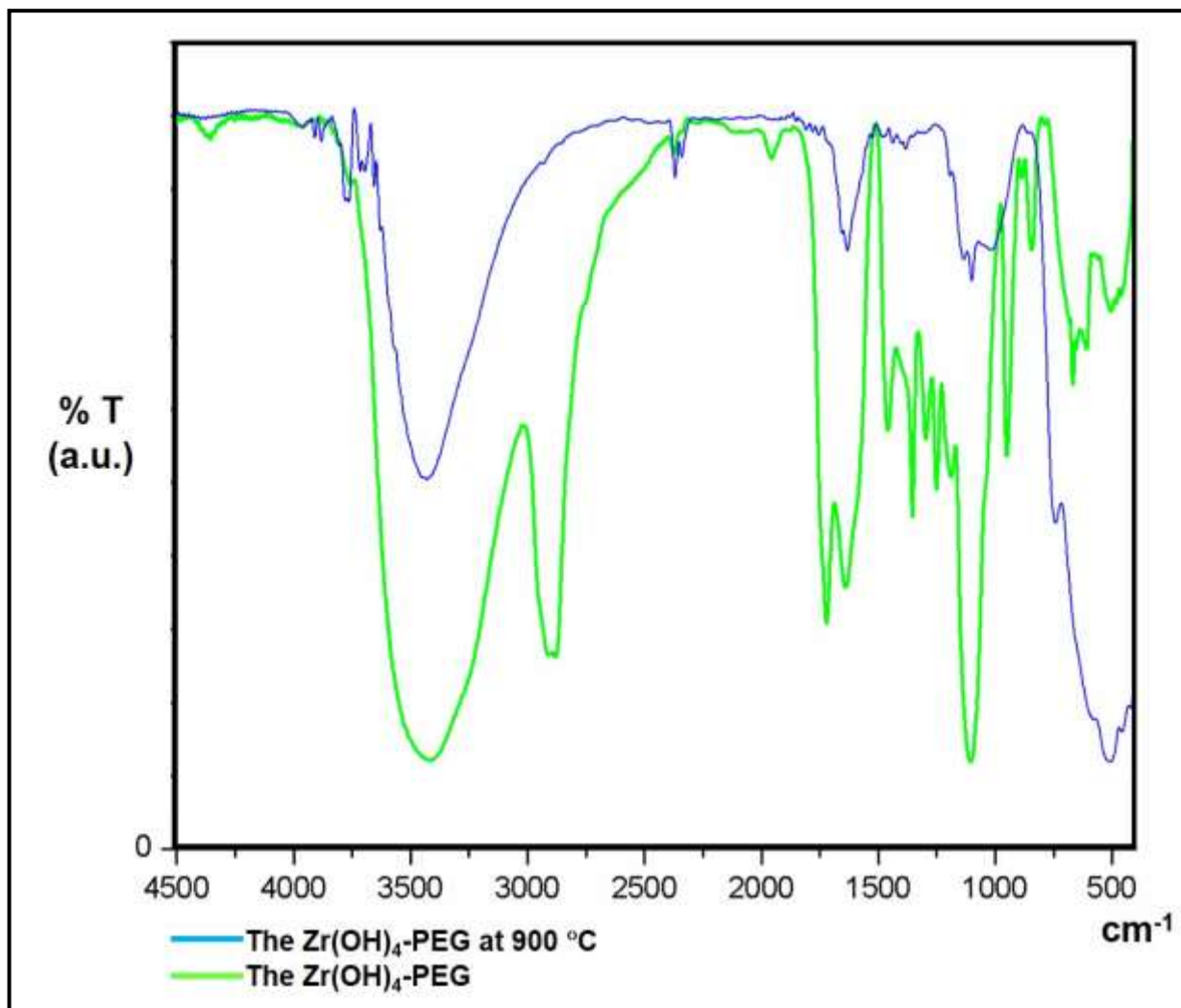
Figure 3: The FT-IR spectra of the Zr(OH)$_4$-PEG samples
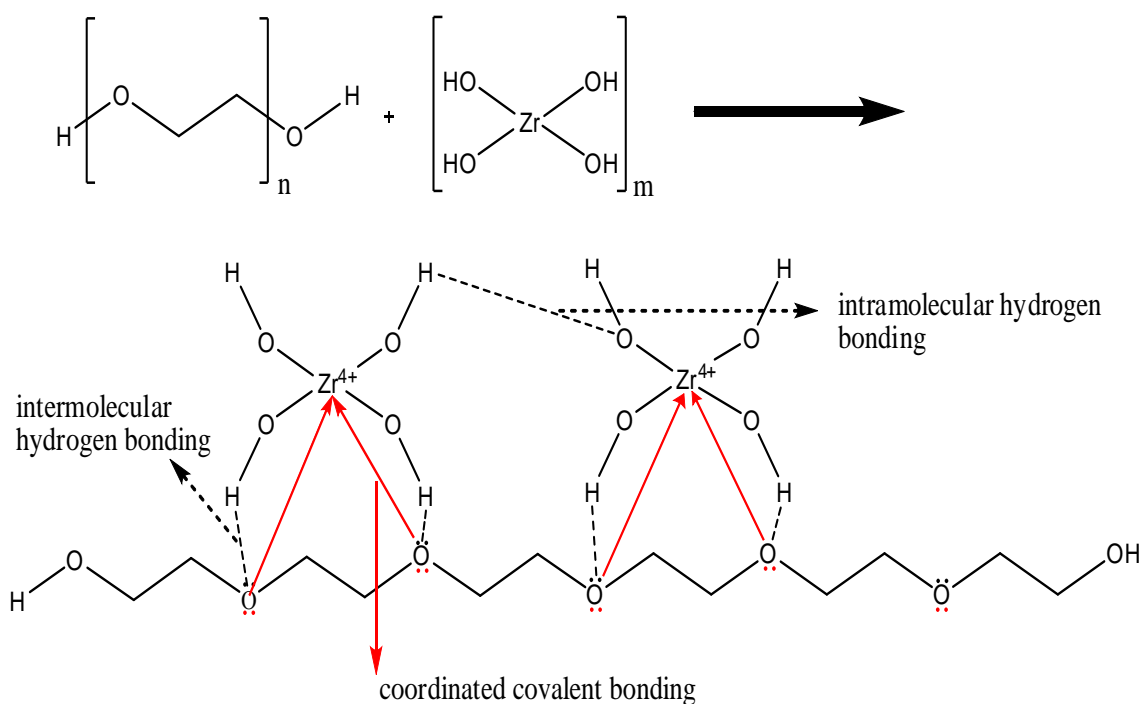
Figure 4: A possible interaction between PEG and Zr(OH)$_4$ during synthesis of ZrO$_2$ 1-D nanomaterials under ultrasound treatment
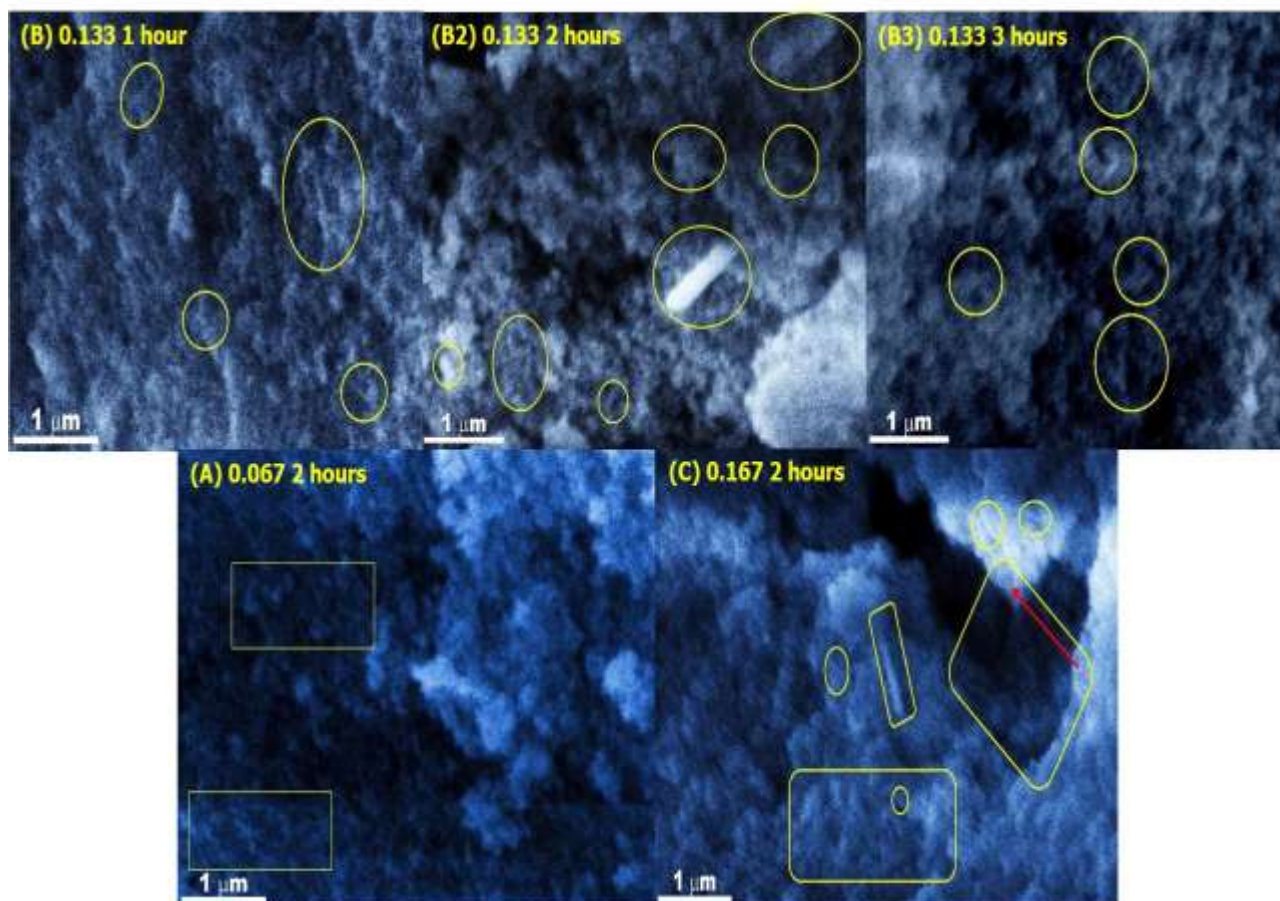
Figure 5: Typical SEM images of the ZrO₂ prepared at various PEG/Zr ratios, at different aging periods and at 900°C

Table 1
Elucidation of FT-IR spectra peaks on the as-synthesized ZrO₂ and the calcined ZrO₂

Elucidation of FT-IR Spectra Peaks	Wavenumber (1/cm)	
	the as-synthesized ZrO_2	ZrO_2 at 900 °C
Various vibrations of the Si-O bonds, are induced from the SiO_2 impurity	462.92, 844.82,	1016.49, 1134.14
Various vibrations of the Zr-O bonds	482.20, 501.49, 609.51, 667.37	420.48, 457.13, 513.07, 576.72, 742.59
Stretching vibration of Zr-OH	1105.21, 1188.15	1099.43
the hydroxyl groups (-OH) on the surface of ZrO_2	1641.42	1631.78
Stretching vibration H–O-H, (intramolecular hydrogen bonding)	3412.08	3446.79
Stretching vibration–O-H, (intermolecular hydrogen bonding), weak shoulder	3235.00	
The C-C stretching vibration of PEG-6000	844.82	
The CH- bending vibration of PEG-6000	1641.42, 1720.50	
The CH_2- bending vibration of PEG-6000	844.82, 950.91, 1460.11	
The CH_2- stretching vibration of PEG-6000	2879.72, 2908.65,	
The CH_2- formation of PEG-6000	950.91,1249.87, 1296.16, 1352.10	
The C-O-C stretching vibration of PEG-6000	1016.49, 1105.21	

*Research Journal of Chemistry and Environment*_____Vol. **22(Special Issue II)** August **(2018)**

Res. J. Chem. Environ.
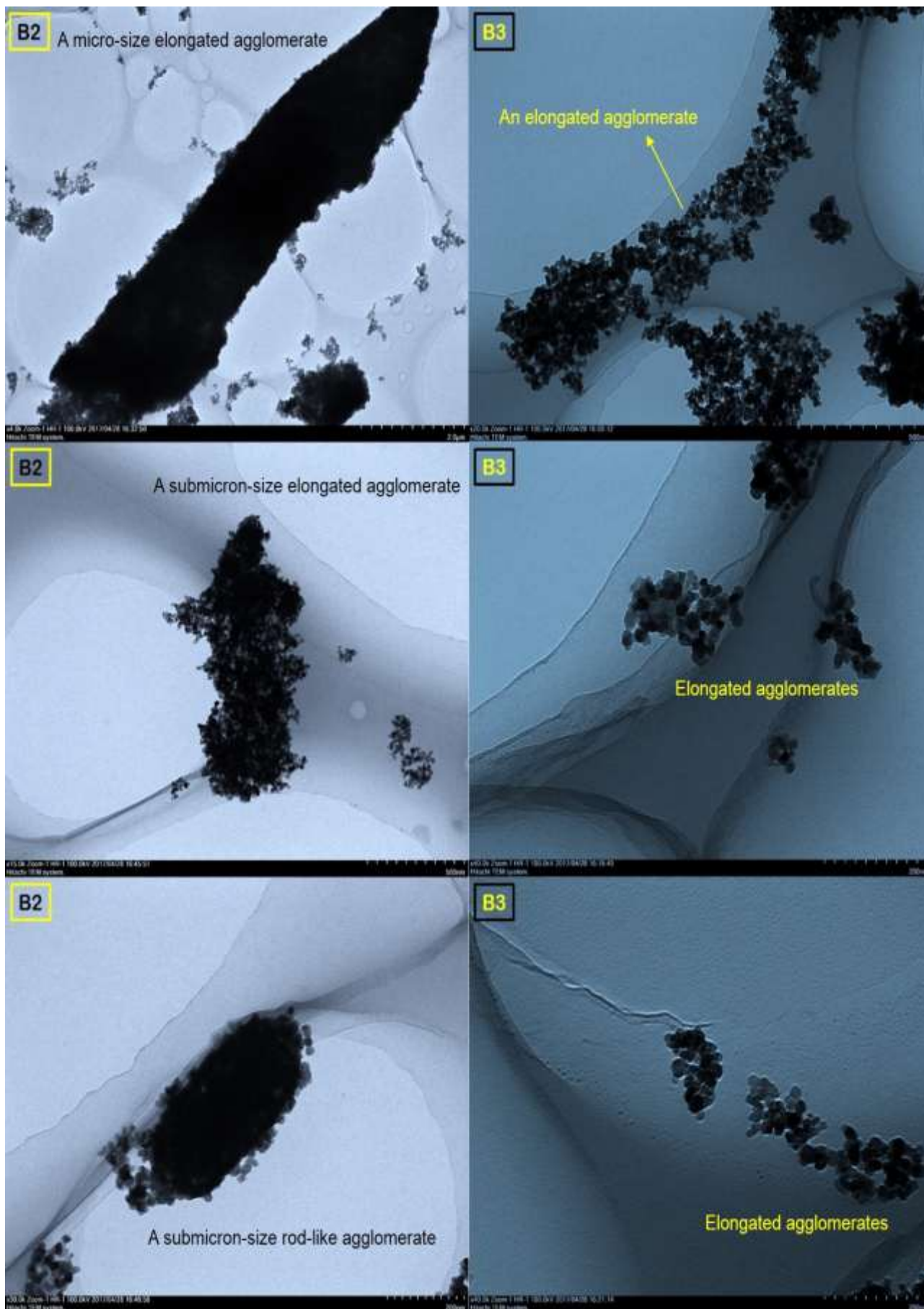
Figure 6: Typical TEM images of the samples B2 and B3 at 900 °C
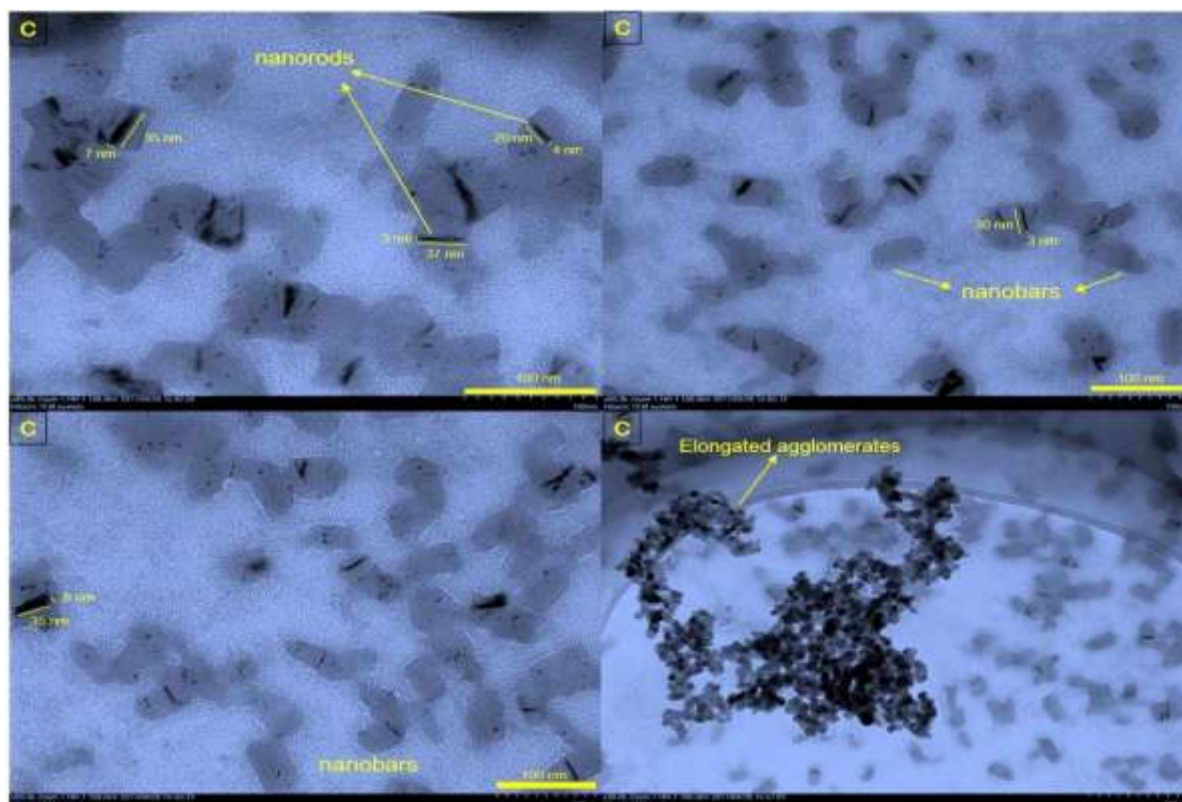
Figure 7: Typical TEM images of a sample C at 900 °C

This phenomenon shows that the longer aging ultrasound period allows the rod-like ZrO_2 particles formed to grow whereby it is evidenced by a sample B2 which consists of a larger 1D-like particle showing approximately 6 μm in length and 1.5 μm in diameter as given by the TEM analysis result in figure 6B2. In addition, the TEM images in figure 6B2 show Ostwald ripening phenomenon in which a large growing 1-D particle attracts other smaller particles. By contrast, since the aging period increased to 3 hours for sample B3, the rod-like ZrO_2 particles are more difficult to be found as shown by SEM in figure 5B3.

Nevertheless, a few of them can still be seen in the SEM image. However, this profile microstructure differs significantly from a sample B2. The TEM analysis result in figure 6B3 shows a microstructure of elongated agglomerates consisting of growing nanoparticles. It is assumed that the aging process for 3 hours in synthesis of a sample B3 has led to high dispersion of particles, allowing well-templated process of $Zr(OH)_4$ by PEG, resulting in the ZrO_2 microstructure similar with the PEG structure.

Figure 7 shows particular TEM images of a sample C at 900°C using a JEM-1400 120 kV TEM. Sample C that was synthesized at the PEG/Zr mole ratio of 0.167 with an aging period for 2 hours has produced ZrO_2 in 1-D structures such as nanorod-like and nanobar-like shapes and elongated agglomerates as shown in figure 7. The nanorod-like particles of ZrO_2 in figure 7 mostly demonstrate a diameter of 3-8 nm and a length of 20-37 nm, with aspect ratios of 4-12. Thus, it belongs to 1-D nanomaterial structure.

Conclusion

In this study, Zirconia 1-D nanomaterials were successfully prepared from local zircon-based $Zr(OH)_4•xH_2O$ mediated by PEG-6000 at various concentrations through an aging ultrasonic method. The result of the study indicated that the crystallization of ZrO_2 occurred at approximately 810°C. Nevertheless, ZrO_2 1-D nanomaterials were obtained in such specific conditions of the PEG/Zr mole ratio of 0.167, at pH 9, at a synthesis temperature of 80°C for 2 hours and at a calcination temperature of 900°C.

The calcined zirconia shows good crystallinity and consists of 64.2% tetragonal and 35.8% monoclinic structures with the average crystal sizes of less than 20 nm. In addition, the ZrO_2 exhibits 1-D morphologies such as nanorod-like shapes with aspect ratios of 4-12, nanobar-like shapes and elongated agglomerates.

Acknowledgement

References
1. Panda P.K., Ceramic nanofibers by electrospinning technique – a Review, *Trans. Ind. Ceram. Soc.*, **66(2)**, 65-76 **(2007)**

2. Xu X., Guo G. and Fan Y., Fabrication and characterization of dense zirconia and zirconia silica ceramic nanofibers, *J. Nanosci. Nanotechnol.*, **10(9)**, 5672-5679 **(2010)**

3. Jirsak O., Nanofibers, technology and applications, http://www.fzu.cz/~nanoteam/events/ws2006/jirsak, accessed on 27 August **(2013)**

4. Maryani E., Subagjo Nuruddin A., Septawendar R. and Purwasasmita B.S., Effects of aging and temperature parameters, polyethylene glycol (PEG)/Al ratios on the structure directing mechanism of γ-alumina nanofiber-based Indonesian natural kaolin by ultrasonic aging process, *Journal of The Australian Ceramic Society*, **51(2)**, 116 – 122 **(2015)**

5. Azad A.M., Fabrication of yttria stabilized zirconia nanofibers by electrospinning, *Material Letters*, **60**, 67-72 **(2006)**

6. Guo G., Fan Y., Zhang J.F., Hagan J.L. and Xu X., Novel dental composites reinforced with zirconia–silica ceramic nanofibers, *Dental Materials*, **28**, 360-368 **(2012)**

7. Wang J., Jin E.M., Park J.Y., Wang W.L., Zhao X.G. and Gu H.B., Increases in solar conversion efficiencies of the ZrO_2 nanofiber-doped TiO_2 photoelectrode for dye-sensitized solar cells, *Nanoscale Research Letters*, **7**, 1-4 **(2012)**

8. Xu H., Qin D.H., Yang Z. and Li H.L., Fabrication and characterization of highly ordered zirconia nanowire arrays by sol–gel template method, *Materials Chemistry and Physics*, **80**, 524–528 **(2003)**

9. Tsai M.C., Lin G.T., Chiu H.T. and Lee C.Y., Synthesis of zirconium dioxide nanotubes, nanowires and nanocables by concentration dependent solution deposition, *J Nanopart. Res.*, **10**, 863–869 **(2008)**

10. Dong W.S., Lin F.Q., Liu C.L. and Li M.Y., Synthesis of ZrO_2 nanowires by ionic-liquid route, *Journal of Colloid and Interface Science*, **333**, 734–740 **(2009)**

11. Chu S.Z., Wada K., Inoue S. and Segawa H., Direct growth of highly ordered crystalline zirconia nanowire arrays with high aspect ratios on glass by a tailored anodization, *Journal of The Electrochemical Society*, **158(5)**, C148-C157 **(2011)**

12. Chen Y., Gu J., Zhub S., Sub H., Zhang D., Feng C. and Zhuang L., Synthesis of naturally cross-linked polycrystalline ZrO_2 hollow nanowires using butterfly as templates, *Materials Chemistry and Physics*, **134**, 16–20 **(2012)**

13. Khan S.A., Fu Z., Rehman S.S., Asif M., Wang W. and Wang H., Study of template-free synthesis hierarchical m-ZrO_2 nanorods by hydrothermal method, *Powder Technology*, **256**, 71–74 **(2014)**

14. Maryani E., Abdullah M., Damayanti H. and Septawendar R., Effect of ultrasonic irradiation on the characteristics of γ-Al_2O_3 nanorods synthesized from nitrate salt-starch precursors through a facile precipitation method, *Journal of the Ceramic Society of Japan*, **124(12)**, 1205-1210 **(2016)**

15. Septawendar R., Nuruddin A., Sutardi S., Maryani E., Asri L.A.T.W. and Purwasasmita B.S., Low-temperature metastable tetragonal zirconia nanoparticles (NpMTZ) synthesized from local zircon by a modified sodium carbonate sintering method, *Journal of the Australian Ceramic Society*, https://doi.org/10.1007/s41779-018-0193-4 **(2018)**

16. Lin Z., Han X., Wang T. and Li S., Effects of adding nano metal powders on thermooxidative degradation of poly(ethylene glycol), *Journal of Thermal Analysis and Calorimetry*, **91(3)**, 709–714 **(2008)**

17. Han S., Kim C. and Kwon D., thermal/oxidative degradation and stabilization of polyethylene glycol, *Polymer*, **38(2)**, 317-323 **(1997)**

18. Heshmatpour F. and Aghakhanpour R.B., Synthesis and characterization of nanocrystalline zirconia powder by simple sol–gel method with glucose and fructose as organic additives, *Powder Technology*, **205**, 193–200 **(2011)**

19. Heshmatpour F. and Aghakhanpour R.B., Synthesis and characterization of superfine pure tetragonal nanocrystalline sulfated zirconia powder by a non-alkoxide sol–gel route, *Advanced Powder Technology*, **23**, 80–87 **(2012)**

20. Glover T.G., Peterson G.W., DeCoste J.B. and Browe M.A., Adsorption of ammonia by sulfuric acid treated zirconium hydroxide, *Langmuir*, **28**, 10478−10487 **(2012)**

21. Raghavendra V.B., Naik S., Antony M., Ramalingam G., Rajamathi M. and Raghavan S., Amorphous, monoclinic and tetragonal porous zirconia through a controlled self-sustained combustion route, *J. Am. Ceram. Soc.*, **94(6)**, 1747–1755 **(2011)**

22. Sarkar D., Mohapatra D., Ray S., Bhattacharyya S., Adak S. and Mitra N., Synthesis and characterization of sol–gel derived ZrO_2 doped Al_2O_3 nanopowder, *CERIN*, **33**, 1275-1282 **(2007)**

23. Septawendar R., Sutardi S., Purwasasmita B.S. and Edwin F., Preparation of nanocrystalline ZrO_2 powder via a chemical route, *Journal of the Australian Ceramics Society*, **48(1)**, 12-20 **(2012)**

24. Ortiz-Landeros J., Contreras-García M.E. and Pfeiffer H., Tailored macroporous ZrO_2-Al_2O_3 mixed oxides by template-assisted method: novel materials for catalytic applications, *Azojomo*, **4**, 1-11 **(2008)**

25. Tyagi B., Sidhpuria K., Shaik B. and Vir Jasra R., Synthesis of nanocrystalline zirconia using sol-gel and precipitation techniques: "Materials and Interfaces, *Ind. Eng. Chem. Res.*, **45**, 8643-8650 **(2006)**

26. Abu-Zied B.M., Hussein M.A. and Asiri A.M., Characterization, *In situ* electrical conductivity and thermal behavior of immobilized PEG on MCM-41, *Int. J. Electrochem. Sci.*, **10**, 4873–4887 **(2015)**.